

EXTREME GAS FRACTIONS IN CLUMPY, TURBULENT DISK GALAXIES AT $Z \sim 0.1$

DAVID B. FISHER¹, KARL GLAZEBROOK^{1,2}, ALBERTO BOLATTO³, DANAIL OBRESCHKOW^{2,4}, ERIN MENTUCH COOPER⁵, EMILY WISNIOSKI⁶, ROBERT BASSETT¹, ROBERTO G. ABRAHAM⁷, IVANA DAMJANOV⁸, ANDY GREEN⁹, PETER MCGREGOR¹⁰

¹Centre for Astrophysics and Supercomputing, Swinburne University of Technology, P.O. Box 218, Hawthorn, VIC 3122, Australia

²ARC Centre of Excellence for All-sky Astrophysics (CAASTRO)

³Laboratory of Millimeter Astronomy, University of Maryland, College Park, MD 29742

⁴International Centre for Radio Astronomy Research (ICRAR), M468, University of Western Australia, 35 Stirling Hwy, Crawley, WA 6009, Australia

⁵Department of Astronomy, The University of Texas at Austin, Austin, TX 78712, USA

⁶Max Planck Institute for Extraterrestrial Physics, Garching, Germany

⁷Department of Astronomy & Astrophysics, University of Toronto, 50 St. George St., Toronto, ON M5S 3H8, Canada

⁸Harvard-Smithsonian Center for Astrophysics, 60 Garden St., Cambridge, MA 02138, USA

⁹Australian Astronomical Observatory, P.O. Box 970, North Ryde, NSW 1670, Australia and

¹⁰Research School of Astronomy and Astrophysics, Australian National University, Cotter Rd, Weston, ACT 2611, Australia

Draft version June 13, 2022

ABSTRACT

In this letter we report the discovery of CO fluxes, suggesting very high gas fractions in three disk galaxies seen in the nearby Universe ($z \sim 0.1$). These galaxies were investigated as part of the DYNAMO of Newly-Assembled Massive Objects (DYNAMO) survey. High-resolution Hubble Space Telescope imaging of these objects reveals the presence of large star forming clumps in the bodies of the galaxies, while spatially resolved spectroscopy of redshifted $H\alpha$ reveals the presence of high dispersion rotating disks. The internal dynamical state of these galaxies resembles that of disk systems seen at much higher redshifts ($1 < z < 3$). Using CO(1-0) observations made with the Plateau de Bure Interferometer, we find gas fractions of 20-30% and depletion times of $t_{dep} \sim 0.5$ Gyr (assuming a Milky Way-like α_{CO}). These properties are unlike those expected for low-redshift galaxies of comparable specific star formation rate, but they are normal for their high- z counterparts. DYNAMO galaxies break the degeneracy between gas fraction and redshift, and we show that the depletion time per specific star formation rate for galaxies is closely tied to gas fraction, independent of redshift. We also show that the gas dynamics of two of our local targets corresponds to those expected from unstable disks, again resembling the dynamics of high- z disks. These results provide evidence that DYNAMO galaxies are local analogues to the clumpy, turbulent disks, which are often found at high redshift.

Subject headings:

1. INTRODUCTION

In the past decade surveys have shown that there is a decline at lower redshifts in both star formation (Madau et al. 1996; Hopkins & Beacom 2006) and the average fraction of molecular gas mass in galaxies (Tacconi et al. 2010; Combes et al. 2013; Carilli & Walter 2013). Observations show that ionized gas in $1 < z < 5$ galaxies tends to be very clumpy (eg. Swinbank et al. 2009; Genzel et al. 2011). These clumps are very massive ($\sim 10^9 M_{\odot}$), and they are forming impressive numbers of stars ($\lesssim 10 M_{\odot} \text{ yr}^{-1}$). A large fraction of clumpy galaxies have dynamics that are consistent with a rotating disk in which the gas is also turbulent (eg. Förster Schreiber et al. 2009; Wisnioski et al. 2011). CO observations of these galaxies indicate very high molecular gas fractions, $f_{gas} \sim 20-50\%$ (e.g. Tacconi et al. 2010). Much remains unknown about clumpy galaxies (for a recent review see Glazebrook 2013), largely because they are almost exclusively found at high redshift, and are thus quite difficult to observe.

Using data from the DYNAMO (DYNAMICS of Newly-Assembled Massive Objects) survey, Green et al. (2010) report the discovery of a sample of galaxies at $z \sim 0.1$ whose properties closely match those of high redshift, clumpy disk galaxies. The DYNAMO dataset includes integral field observations of $H\alpha$ in 95 spiral galaxies with the highest $H\alpha$ luminosities ($L_{H\alpha} > 10^{40} \text{ erg s}^{-1}$) in the Sloan Digital Sky

Survey (SDSS), after excluding AGN from the sample. Kinematic maps of over 80% of DYNAMO galaxies show signs of rotation, and in over half of the sample that rotation is consistent with the Tully-Fisher relation (Green et al. 2013). Most DYNAMO galaxies have large internal velocity dispersions $\sigma \sim 10-100 \text{ km s}^{-1}$.

If clumpy disk galaxies are dynamically unstable then a high gas fraction is needed in these systems that also have high internal velocity dispersions (e.g. Bournaud et al. 2014). Very high gas fractions are observed in distant clumpy systems (Tacconi et al. 2013), reinforcing the view that global Toomre instabilities may be important in these objects. In this letter we report the results from new observations from Plateau de Bure Interferometer (PdBI), which confirm high gas fractions in three DYNAMO galaxies.

2. METHODS

2.1. Observations & Flux Measurements

The DYNAMO sample was selected from the Sloan Digital Sky Survey (York & SDSS Collaboration 2000), and is comprised of 95 galaxies of known stellar mass with integral field spectroscopy (around the $H\alpha$ line) obtained from the Anglo-Australian Telescope. We refer the reader to Green et al. (2013) for details.

Observations centered on CO(1-0) were made for four DYNAMO galaxies with the Plateau de Bure Interferometer (PdBI). Three of these were recovered with significant detections. The systems observed were D 13-5, G 04-1, G 10-

1 and H 10-2. Stellar masses for these systems range from $1-7 \times 10^{10} M_{\odot}$ and redshifts span the range $z = 0.075-0.15$. Star formation rates for D 13-5, G 10-1 and H 10-2 are $\sim 20 \pm 10 M_{\odot} \text{ yr}^{-1}$. The star formation rate of G 04-1 is somewhat higher at $50 \pm 10 M_{\odot} \text{ yr}^{-1}$. Galaxies G 04-1 and D 13-5 are classified as rotating disks, while H 10-2 and G 10-1 are classified as a perturbed rotators due to asymmetries in their velocity fields, and may be experiencing merging.

Observations described here were made using the PdBI in D configuration (FWHM $\sim 6''$) from 30-May-2013 to 16-July-2013. On-source integration times were 1-2 hours per target. Data were calibrated and reduced with standard methods at IRAM. The spectra were binned into 20 km s^{-1} channels. Fluxes were measured, using standard GILDAS routines, by defining an ellipse in the moment zero CO(1-0) map (the outer contour in Fig. 1). The noise levels are $0.31 \text{ Jy km s}^{-1}$ (D 13-5), $0.48 \text{ Jy km s}^{-1}$ (G 04-1), $0.26 \text{ Jy km s}^{-1}$ (G 10-1) and $0.42 \text{ Jy km s}^{-1}$ (H 10-2).

On three of our sources we recovered significant detections. We do not find a statistically significant flux for H 10-2, our most distant source, but find an upper limit consistent with the gas fractions measured in the other three galaxies (see Section 3). Data for each detected galaxy is shown Fig. 1. The flux measurements on D 13-5, G 04-1, G10-1 have $S/N \sim 30, 13$ and 6 , respectively.

In Fig. 2 we show $H\alpha$ maps of two of our target galaxies, D 13-5 and G 04-1, obtained using the Advanced Camera for Surveys (ACS) ramp filters on the Hubble Space Telescope (HST; PID 12977, PI Damjanov). The DYNAMO galaxies shown have a clumpy distribution of ionized gas, and their appearance in $H\alpha$ is remarkably similar to that seen in many high-redshift galaxies (e.g. Genzel et al. 2011; Wisnioski et al. 2012) and simulations of clumpy galaxies (Bournaud et al. 2014). These galaxies both show evidence of a ring of gas, similar to that of high- z galaxies (Genzel et al. 2008, 2011, 2014). Though we note that gas rings are common in low- z non-turbulent, often barred, galaxies as well (eg. Böker et al. 2008). Individual clumps have very bright $H\alpha$ emission, implying star formation rates of individual clumps $\sim 1-10 M_{\odot} \text{ yr}^{-1}$. Surveys of high- z lensed galaxies, in which the clump sizes are not limited by resolution, find that clumps are typically 100-400 pc (Jones et al. 2010). This is consistent with the sizes of clumps in our target galaxies. A detailed analysis of the clump properties from a larger sample of HST images will be the subject of a future paper (Fisher et al. *in prep*).

2.2. Conversion to total molecular gas

The conversion of CO(1-0) flux to total molecular gas mass was done in the usual fashion, where

$$M_{\text{mol}} = \alpha_{\text{CO}} L_{\text{CO}}. \quad (1)$$

The quantity L_{CO} represents the luminosity of CO(1-0), and α_{CO} is the conversion factor of CO-to- H_2 (including the $1.36\times$ factor accounting for Helium). Typical values for α_{CO} range from $0.8-4.5 M_{\odot} \text{ pc}^{-2} (\text{K km s}^{-1})^{-1}$. For discussion of this conversion factor in different environments see Young & Scoville 1991; Downes & Solomon 1998; Fisher et al. 2012 and Bolatto et al. (2013) for a detailed review.

G 04-1 and D 13-5 have $H\alpha$ kinematics that indicate rotating systems (Green et al. 2013), and the surface brightness profile of the star light in SDSS images closely resembles an exponential disk with at most a small (B/T<10%) bulge. It

therefore seems reasonable to assume a conversion factor similar to the Milky Way (as done by Tacconi et al. 2013). However, the large star formation rates in these galaxies suggest that a smaller conversion factor ($\alpha_{\text{CO}} \sim 1$) may be appropriate. Bolatto et al. (2013) provides a first estimate for a universal equation to determine the CO-to- H_2 conversion factor in galaxies, such that

$$\alpha_{\text{CO}} \approx 2.9 \exp\left(\frac{0.4}{Z' \Sigma_{\text{GMC}}^{100}}\right) \left(\frac{\Sigma_{\text{total}}}{100 M_{\odot} \text{ pc}^{-2}}\right)^{-0.5} \quad (2)$$

where Z' represents the metallicity in solar units, $\Sigma_{\text{GMC}}^{100}$ represents the average surface density of molecular clouds in units of $100 M_{\odot} \text{ pc}^{-2}$, and Σ_{total} is the total surface density of the region in question. We find that metallicities fall in the range $Z' \sim 0.9-1.1$, using the [NII]/ $H\alpha$ ratio (Pettini & Pagel 2004) from SDSS spectra. The average surface density of molecular clouds in these clumpy galaxies is presently uncertain. Star forming clumps may be as massive as $10^9 M_{\odot}$ and have radii $R_{\text{clump}} \sim 500 \text{ pc}$ (Swinbank et al. 2012), which yields $\Sigma_{\text{GMC}}^{100} \sim 10$. The total surface densities of our galaxies are $100-300 M_{\odot} \text{ pc}^{-2}$, measured from SDSS surface photometry. Inserting these quantities into Equation 2 results in $\alpha_{\text{CO}} \sim 3.1 M_{\odot} \text{ pc}^{-2} (\text{K km s}^{-1})^{-1}$ for our targets. This value is adopted for α_{CO} . We note that our chosen α_{CO} is consistent with estimates of α_{CO} in the Milky Way (eg. Dame et al. 2001).

We do not currently have sufficient data to measure the temperature of the gas in these galaxies, though indirect evidence supports our choice of disk-like α_{CO} . Mentuch-Cooper et al. (*in prep*) find with *Herschel* data that in similar DYNAMO galaxies the dust temperatures are $T_{\text{dust}} \sim 25-35 \text{ K}$, which is consistent with $\alpha_{\text{CO}} \sim 3-4$ (Magnelli et al. 2012). Also, connections between ISM state and mid-plane pressure in galaxies (Blitz & Rosolowsky 2006), suggest a link between gas temperature and total surface density. It is therefore likely that using surface density implicitly accounts for gas temperature. Nonetheless, in light of the well-known uncertainties of CO-to- H_2 conversion in such high star formation systems, for our main result (Fig. 3), we show $L_{\text{CO}}/M_{\text{star}}$ along with the more physical gas fraction.

We use variable α_{CO} from Bolatto et al. (2013) to adjust the gas masses of our comparison samples. For the COLD GASS galaxies we estimate the stellar surface density with stellar masses and sizes given in Saintonge et al. (2011a); we assume $\Sigma_{\text{GMC}}^{100} \approx 1.7$ (Bolatto et al. 2008) and $Z' \approx 1$. For (Saintonge et al. 2011a) galaxies the typical adjustment is very minor. The ultra luminous infrared galaxies (ULIRGs) from Combes et al. (2013) require $\alpha_{\text{CO}} = 0.8$, and thus these gas masses do not change.

We make the same assumptions about $\Sigma_{\text{GMC}}^{100}$ in PHIBSS galaxies as for DYNAMO galaxies, and use published values (Tacconi et al. 2013) for stellar mass and size to estimate the stellar surface density. Gas masses in gas-rich star forming galaxies, are not known to better than a factor of $\sim 2\times$ due to uncertainties in the conversion factor. For the PHIBSS galaxies the gas masses are reduced by 10-40%, by using the variable conversion factor.

3. RESULTS

The gas mass fraction f_{gas} , defined as $f_{\text{gas}} = M_{\text{mol}}/(M_{\text{mol}} + M_{\text{star}})$, of our sample is presented in Fig. 3. The DYNAMO galaxies have $f_{\text{gas}} = 0.18 \pm 0.07, 0.31 \pm 0.03$ and 0.22 ± 0.21 for D 13-5, G 04-1, and G 10-1 respectively. An upper-limit to

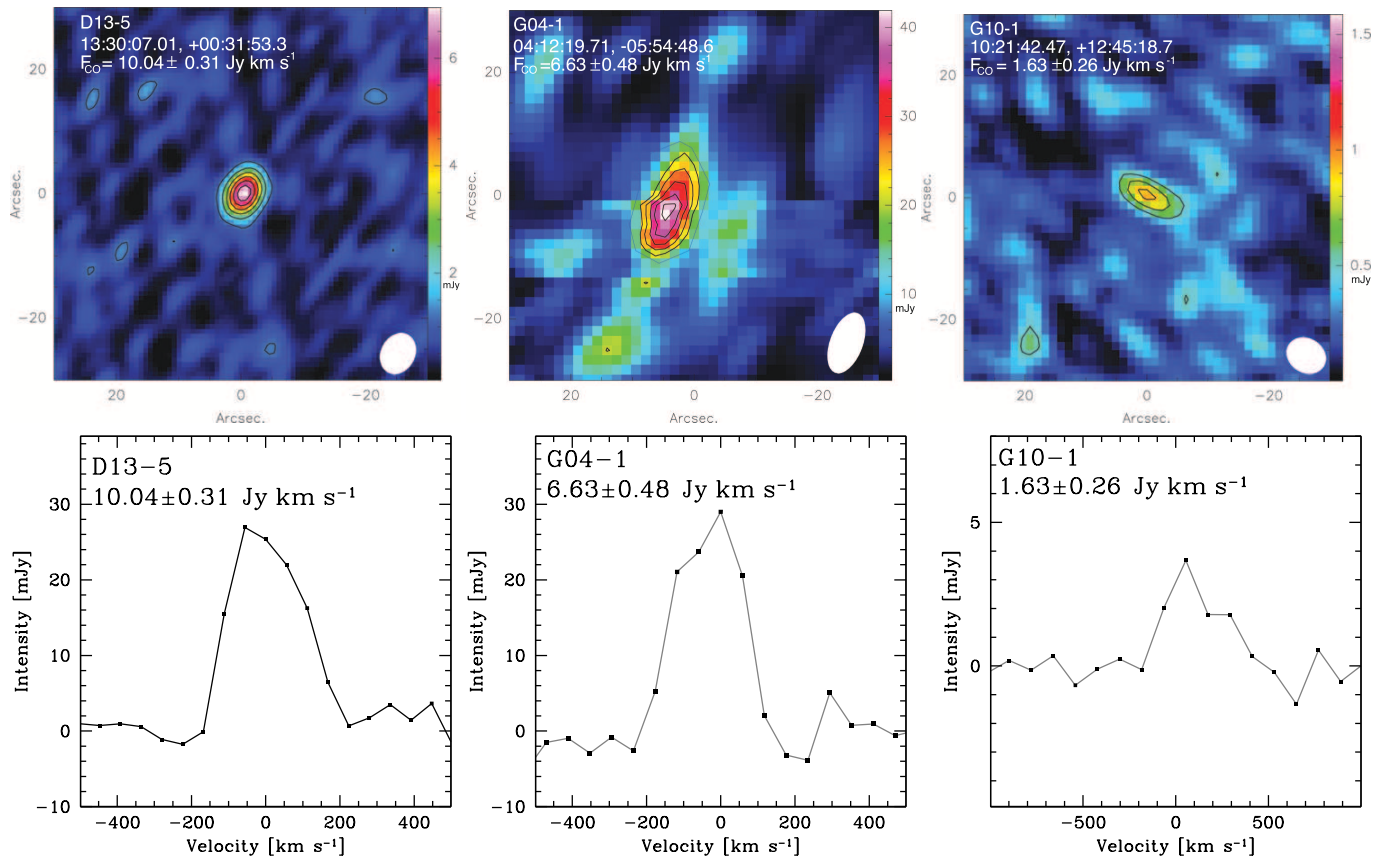


FIG. 1.— Top row: Moment 0 maps of the three galaxies in which we detect CO(1-0) emission. (We do not recover a statistically significant flux on H 10-2). The typical beam size of our observations is 6 arcseconds, beam shapes are shown as the white ellipse in the bottom right corner of each panel. The beam of G 04-1 is very elongated due to the galaxy being lower on the sky. Note that in all cases the CO emission is unresolved, the elongated structure of G 04-1 is due to the low elevation of the observation. The contours are in units of 2σ . Bottom row: Spectra of each detection. In these 3 galaxies, the maps and spectra show clear detections in CO(1-0).

the gas fraction of H 10-2 is $f_{gas} < 0.22$. As it adds essentially no information, the upper-limit of H 10-2 is not displayed in our figures.

Alternatively, if one assumes a starburst like $\alpha_{CO} \sim 1$ the gas fractions are ~ 0.06 , 0.10, and 0.07 for D 13-5, G 04-1, and G 10-1.

From the bottom panel of Fig. 3 it can be seen that our DYNAMO galaxies are more gas rich than typical low redshift galaxies. The histogram in this panel corresponds to the $z \sim 0$ COLD GASS survey (Saintonge et al. 2011a), which is volume limited for galaxies with $M_{star} > 10^{10} M_{\odot}$. Saintonge et al. (2011a) finds that only 5% of low- z galaxies have gas fractions greater than 15% and the median gas fraction for COLD GASS galaxies in which CO is detected is 7% with a standard deviation of $\sim 6\%$.

In the middle panel of Fig. 3 the gas fractions of our target galaxies are compared with those of the ULIRG sample presented by Combes et al. (2013), who measured the gas fractions and star formation efficiency for systems with $L_{FIR} > 10^{12} L_{\odot}$, spanning the redshift range $z = 0.6 - 1.0$. Note that Combes et al. (2013) published stellar masses using the Salpeter IMF, so we multiplied these stellar masses by 0.55 to convert them to the Chabrier (2003) IMF, thus making them consistent with other stellar masses used in this paper. The ULIRG sample has a large range of gas fractions, and in Fig. 3 shows a double-peaked distribution. The gas fractions of our DYNAMO galaxies fall close to the middle of the range spanned by the more gas rich part of the ULIRG sample.

In the top panel of Fig. 3, we show that the gas fractions of our target DYNAMO galaxies are quite similar to those of the main-sequence $z = 1 - 3$ star forming galaxies presented by Tacconi et al. (2013) as part of the PHIBSS survey. PHIBSS targets star forming and starbursting galaxies of the high redshift Universe, many of which have been revealed to clumpy, turbulent systems.

In the right panels of Fig. 3 we show that the ratio of CO luminosity-to-stellar mass, L_{CO}/M_{*} . The results we find here are similar to the right panels, in which we estimate the gas mass. We find that DYNAMO galaxies are at the extreme high end of L_{CO}/M_{*} values when compared to the GASS survey. Also, we find that luminosity of CO gas per unit stellar mass from DYNAMO galaxies is consistent with the center of the distribution of that of PHIBSS galaxies. The high gas fractions, and CO flux ratios, in DYNAMO galaxies are not due to low stellar masses, which span the range from $3 - 7 \times 10^{10} M_{\odot}$, similar to stellar masses found in gas rich PHIBSS galaxies, and much higher than local gas rich dwarfs.

The depletion times ($t_{dep} = M_{gas}/SFR$) of the DYNAMO galaxies observed are 0.4–0.6 Gyr, assuming α_{CO} from Equation 2. ULIRGS are known to have short depletion times (~ 0.01 Gyr, Carilli & Walter 2013) when compared to that of “main-sequence” mode disks (~ 1 Gyr, eg. Leroy et al. 2008; Rahman et al. 2012). Note, that if we assume a lower CO-to-H₂ conversion factor $\alpha_{CO} = 1$ (K km pc⁻¹)⁻¹, the depletion times are 0.1–0.2 Gyr. This value is outside the

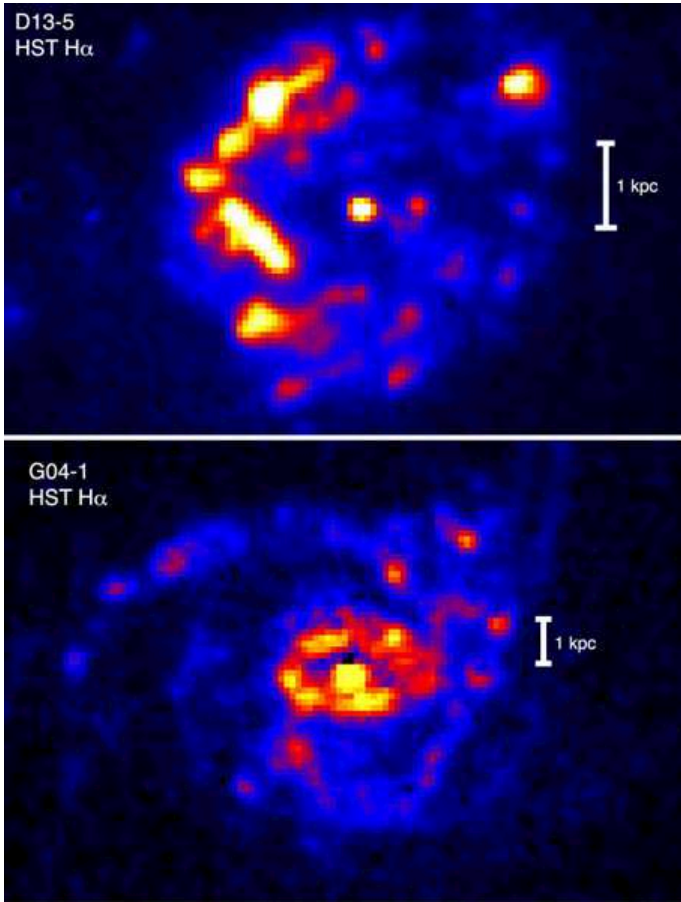


FIG. 2.— HST H α maps of DYNAMO galaxies reveal the presence of massive star forming clumps. Here we show two HST H α maps for our target disk galaxies D 13-5 (top) and G 04-1 (bottom). In each figure the white line indicate 1 kpc. The clumps are of high S/N and have comparable SFR to those observed at high redshift.

range spanned by the Combes et al. (2013) ULIRIG comparison sample (albeit within error bars), and an order of magnitude longer than the median depletion time in the ULIRIG sample.

The relationship between t_{dep} and the specific star-formation rate of a main-sequence disk galaxy changes with redshift (Saintonge et al. 2011b). In the left panel of Fig. 4 we show that there is a strong tendency for galaxies with high gas fractions to have a longer depletion time for a given SFR/M_{star} , including our three galaxies with $f_{gas} \sim 20-30\%$. This is not surprising (see Tacconi et al. 2010), as $t_{dep} \times SFR/M_{star} = M_{gas}/M_{star}$. The correlation with redshift is weaker by comparison, and in the right hand panel we show that the nearby DYNAMO galaxies are clear outliers to the trend, falling in the range populated by $z = 1-2$ galaxies. Also, $\sim 20\%$ (11/51) of galaxies with $z > 1$ are located within the spread of the t_{dep} -specific SFR relationship for $z = 0$ (COLD GASS) galaxies.

In summary, we find that the nearby $z \sim 0.1$ DYNAMO galaxies we target are very similar to the star forming galaxies observed by Tacconi et al. (2013), which are found at $z \sim 1.0-2.5$, in both their gas fractions and depletion times.

4. DISCUSSION

In this paper we report observations that suggest high gas fractions in three nearby clumpy, turbulent galaxies from the DYNAMO sample. Assuming a disk-like CO-to-H $_2$ conver-

sion, the molecular gas fractions ($f_{gas} = M_{mol}/(M_{mol} + M_{star})$) of these three galaxies are $f_{gas} = 20-30\%$. Compared to other low-redshift galaxies, the DYNAMO galaxies are strong outliers: they are gas-rich like $1 < z < 2.5$ galaxies, but they are located in the local Universe. As we show in Fig. 4, the displacement of galaxies, including our target galaxies, from the $t_{dep} - SFR/M_{star}$ relations defined by the local COLD GASS survey is more strongly correlated with gas fraction than it is to redshift. We remind the reader of the caveat that this result depends on the assumption of the disk-like α_{CO} for DYNAMO and PHIBSS galaxies. A straightforward interpretation of our results is that, independent of redshift, having very large gas fraction is a crucial factor to determining a galaxies star forming properties, such as the presence of massive star forming clumps.

Giant star forming clumps, like those in Fig. 2, may be associated with local gravitational instabilities (Genzel et al. 2011; Glazebrook 2013) in disks that are marginally stable (see also Dekel et al. 2009; Bournaud & Elmegreen 2009). Under the assumption that G 04-1 and D 13-5 are disks, and that their clumps are due to turbulent gravitational instabilities, we expect that these galaxies would be unstable as well, and thus have $Q < 1$. We note that an alternate hypothesis, in which G 04-1 and D 13-5 are the result of merging, this calculation would have less meaning, and Q values would be affected by the change to the gas fractions, discussed in § 2 & 3. Similar to Genzel et al. (2011), we express the Toomre (1964) Q parameter as a function of the gas fraction, rotation velocity (V), and velocity dispersion (σ) as follows¹:

$$Q = a \left(\frac{\sigma}{V} \right) \left(\frac{1}{f_{gas}} \right). \quad (3)$$

In the local Universe, typical disks are stable, with $Q \gtrsim 2$ (van der Kruit & Freeman 2011). Taking the dynamical quantities from Green et al. (2013), assuming $a = 1$ for a Keplerian disk and the non-merger conversion CO-to-H $_2$ factor, we measure $Q \sim 0.8$ for D 13-5 and $Q \sim 0.6$ for G 04-1. Assuming these galaxies are truly disks, these results are consistent with a picture in which the clumps observed in DYNAMO galaxies are likely the result of unstable gas.

We conclude by noting the continued similarity between DYNAMO galaxies and turbulent disks seen at high redshifts. Many DYNAMO galaxies have internal dynamical structures similar to those observed in $z \sim 1-2$ galaxies (Förster Schreiber et al. 2009): they are rotating disks with high internal velocity dispersions (Green et al. 2010, 2013). We now add that observations indicate clumpy H α morphologies, high gas fractions, and that they lie on the same portion of the depletion time vs. specific star formation rate diagram occupied by star-forming galaxies at high redshift. Taken together, the evidence continues to be consistent with the hypothesis that DYNAMO galaxies are indeed close analogues to the clumpy galaxies seen at high redshift. In future papers our group will exploit the proximity of DYNAMO to study both high spatial resolution properties of galaxies with massive star forming clumps (Fisher et al. *in prep.*) and the faint stellar kinematics seen in these same galaxies (Bassett et al. *submitted*).

We thank the referee for their helpful comments. We are very grateful to Sabine König for observational support and

¹ For more discussion regarding the measurement of Q in disks, see Leroy et al. (2008), van der Kruit & Freeman (2011) and Glazebrook (2013).

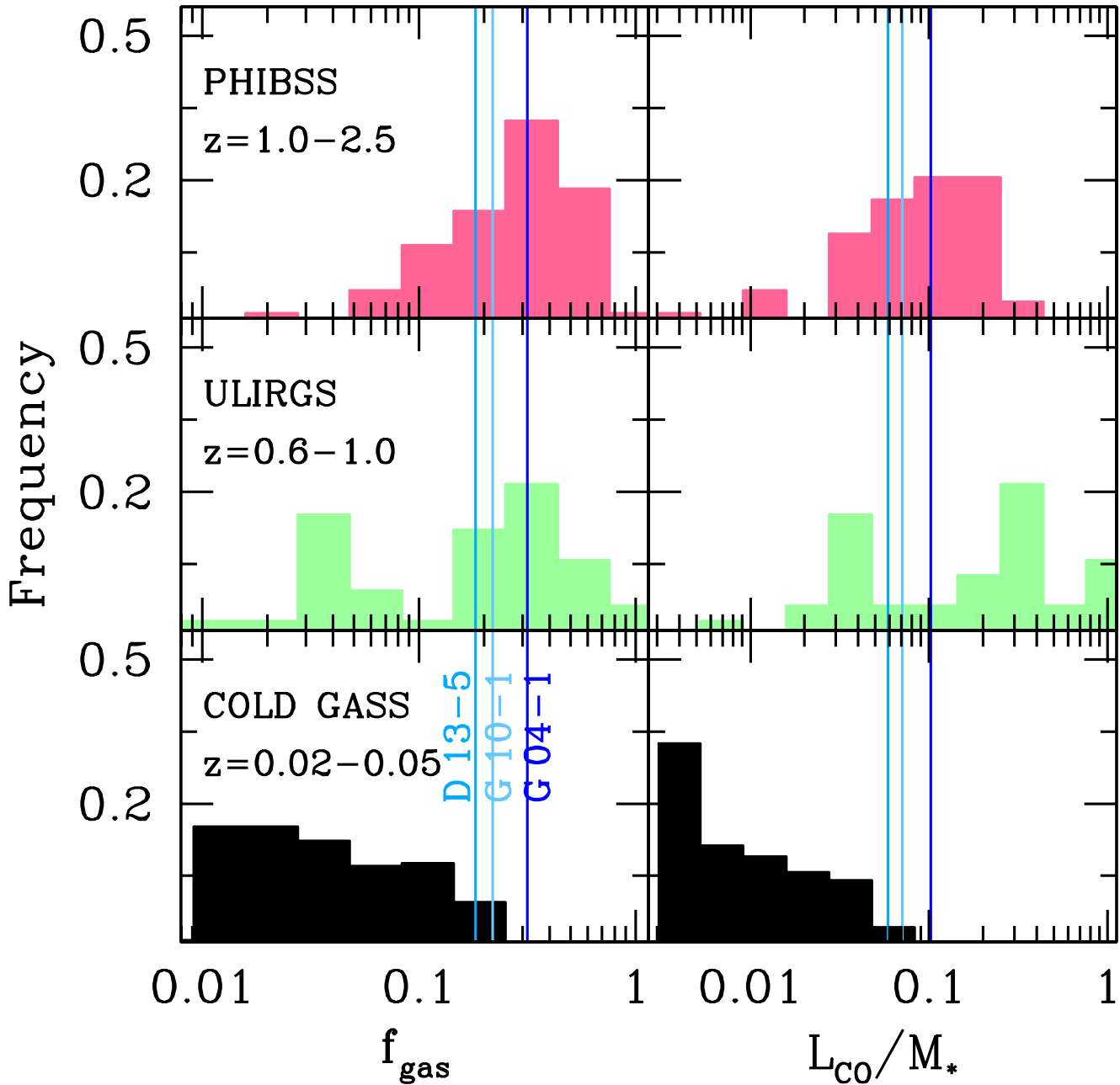


FIG. 3.— A comparison of the gas fractions ($f_{\text{gas}} = M_{\text{mol}}/(M_{\text{mol}} + M_{\text{star}})$) of our target galaxies to the distribution of gas fractions from three surveys at different redshifts. In the right panels we show a similar quantity the ratio of CO luminosity to stellar mass for the same galaxies, a quantity that is independent of assumptions on α_{CO} . From bottom to top, histograms correspond to the GASS survey (Saintonge et al. 2011a) of low redshift galaxies, $z = 0.2-1.0$ ULIRGs from Combes et al. (2013), and the $z = 1.0-2.5$ PHIBSS survey (Tacconi et al. 2013). The gas fractions of our DYNAMO galaxies are indicated by three vertical lines. From left to right, these correspond to D 13-5 (cyan), G 10-1 (light blue) and G 04-1 (dark blue). The DYNAMO galaxies, especially G 04-1, have high gas fractions compared to other galaxies at $z = 0-0.1$, and are much more consistent with star forming galaxies that are found at high redshifts.

help calibrating the data. This work is based on observations carried out with the IRAM Plateau de Bure Interferometer. IRAM is supported by INSU/CNRS (France), MPG (Germany) and IGN (Spain).

DBF acknowledges support from Australian Research Council (ARC) Discovery Program (DP) grant DP130101460. Support for this project is provided in part by

the Victorian Department of State Development, Business and Innovation through the Victorian International Research Scholarship (VIRS). AB acknowledges partial support from AST 08-38178, CAREER award AST 09-55836, and a Cottrell Scholar award from the Research Corporation for Science Advancement.

REFERENCES

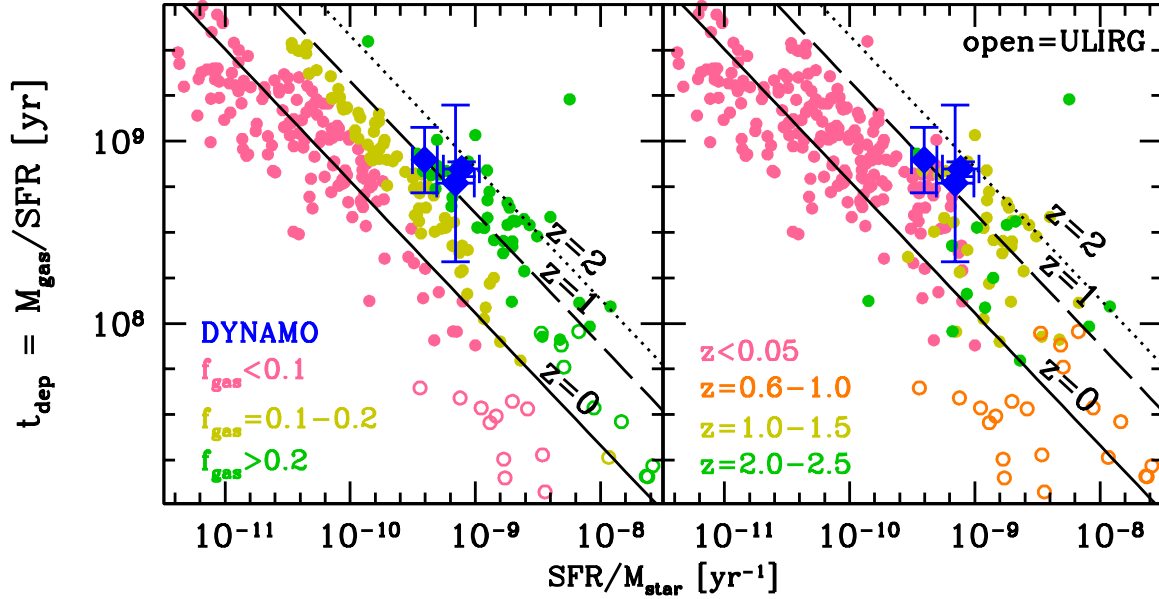


FIG. 4.— The star formation in DYNAMO galaxies is consistent with that of other gas rich main-sequence galaxies. This figure compares the depletion time ($M_{\text{gas}}/\text{SFR}$) to the specific star formation rate. Open symbols represent ULIRGs, while closed symbols are main-sequence disks. In the left panel we organize the symbols based on molecular gas fraction. In the right panel symbol colors are based on redshift. The solid line is the relationship from the COLD GASS survey (Saintonge et al. 2011a), and the higher redshift lines simply adjust that relation by a constant offset based on the measured evolution of the specific SFR with redshift (Pérez-González et al. 2008).

- Bolatto, A. D., Leroy, A. K., Rosolowsky, E., Walter, F., & Blitz, L. 2008, *ApJ*, 686, 948
- Bolatto, A. D., Wolfire, M., & Leroy, A. K. 2013, *ARA&A*, 51, 207
- Bournaud, F., & Elmegreen, B. G. 2009, *ApJ*, 694, L158
- Bournaud, F., Perret, V., Renaud, F., Dekel, A., Elmegreen, B. G., Elmegreen, D. M., Teyssier, R., Amram, P., Daddi, E., Duc, P.-A., Elbaz, D., Epinat, B., Gabor, J. M., Juneau, S., Kraljic, K., & Le Floch, E. 2014, *ApJ*, 780, 57
- Carilli, C. L., & Walter, F. 2013, *ARA&A*, 51, 105
- Chabrier, G. 2003, *PASP*, 115, 763
- Combes, F., García-Burillo, S., Braine, J., Schinnerer, E., Walter, F., & Colina, L. 2013, *A&A*, 550, A41
- Dame, T. M., Hartmann, D., & Thaddeus, P. 2001, *ApJ*, 547, 792
- Dekel, A., Birboim, Y., Engel, G., Freundlich, J., Goerdt, T., Mumcuoglu, M., Neistein, E., Pichon, C., Teyssier, R., & Zinger, E. 2009, *Nature*, 457, 451
- Downes, D., & Solomon, P. M. 1998, *ApJ*, 507, 615
- Fisher, D. B., Bolatto, A. Drory, N., Combes, F., Blitz, L., & Wong, T. 2012, Submitted To *ApJ*
- Förster Schreiber, N. M., Genzel, R., Bouché, N., Cresci, G., Davies, R., Buschkamp, P., Shapiro, K., Tacconi, L. J., Hicks, E. K. S., Genel, S., Shapley, A. E., Erb, D. K., Steidel, C. C., Lutz, D., Eisenhauer, F., Gillessen, S., Sternberg, A., Renzini, A., Cimatti, A., Daddi, E., Kurk, J., Lilly, S., Kong, X., Lehnert, M. D., Nesvadba, N., Verma, A., McCracken, H., Arimoto, N., Mignoli, M., & Onodera, M. 2009, *ApJ*, 706, 1364
- Genzel, R., Burkert, A., Bouché, N., Cresci, G., Förster Schreiber, N. M., Shapley, A., Shapiro, K., Tacconi, L. J., Buschkamp, P., Cimatti, A., Daddi, E., Davies, R., Eisenhauer, F., Erb, D. K., Genel, S., Gerhard, O., Hicks, E., Lutz, D., Naab, T., Ott, T., Rabien, S., Renzini, A., Steidel, C. C., Sternberg, A., & Lilly, S. J. 2008, *ApJ*, 687, 59
- Genzel, R., Förster Schreiber, N. M., Lang, P., Tacchella, S., Tacconi, L. J., Wuyts, S., Bandara, K., Burkert, A., Buschkamp, P., Carollo, C. M., Cresci, G., Davies, R., Eisenhauer, F., Hicks, E. K. S., Kurk, J., Lilly, S. J., Lutz, D., Mancini, C., Naab, T., Newman, S., Peng, Y., Renzini, A., Shapiro Griffin, K., Sternberg, A., Vergani, D., Wisnioski, E., Wuyts, E., & Zamorani, G. 2014, *ApJ*, 785, 75
- Genzel, R., Newman, S., Jones, T., Förster Schreiber, N. M., Shapiro, K., Genel, S., Lilly, S. J., Renzini, A., Tacconi, L. J., Bouché, N., Burkert, A., Cresci, G., Buschkamp, P., Carollo, C. M., Ceverino, D., Davies, R., Dekel, A., Eisenhauer, F., Hicks, E., Kurk, J., Lutz, D., Mancini, C., Naab, T., Peng, Y., Sternberg, A., Vergani, D., & Zamorani, G. 2011, *ApJ*, 733, 101
- Glazebrook, K. 2013, ArXiv e-prints
- Green, A. W., Glazebrook, K., McGregor, P. J., Abraham, R. G., Poole, G. B., Damjanov, I., McCarthy, P. J., Colless, M., & Sharp, R. G. 2010, *Nature*, 467, 684
- Green, A. W., Glazebrook, K., McGregor, P. J., Damjanov, I., Wisnioski, E., Abraham, R. G., Colless, M., Sharp, R. G., Crain, R. A., Poole, G. B., & McCarthy, P. J. 2013, *MNRAS*
- Hopkins, A. M., & Beacom, J. F. 2006, *ApJ*, 651, 142
- Jones, T. A., Swinbank, A. M., Ellis, R. S., Richard, J., & Stark, D. P. 2010, *MNRAS*, 404, 1247
- Leroy, A. K., Walter, F., Brinks, E., Bigiel, F., de Blok, W. J. G., Madore, B., & Thornley, M. D. 2008, *AJ*, 136, 2782
- Madau, P., Ferguson, H. C., Dickinson, M. E., Giavalisco, M., Steidel, C. C., & Fruchter, A. 1996, *MNRAS*, 283, 1388
- Magnelli, B., Saintonge, A., Lutz, D., Tacconi, L. J., Berta, S., Bournaud, F., Charmandaris, V., Dannerbauer, H., Elbaz, D., Förster-Schreiber, N. M., Graciá-Carpio, J., Ivison, R., Maiolino, R., Nordon, R., Popesso, P., Rodighiero, G., Santini, P., & Wuyts, S. 2012, *A&A*, 548, A22
- Pérez-González, P. G., Trujillo, I., Barro, G., Gallego, J., Zamorano, J., & Conselice, C. J. 2008, *ApJ*, 687, 50
- Pettini, M., & Pagel, B. E. J. 2004, *MNRAS*, 348, L59
- Rahman, N., Bolatto, A. D., Xue, R., Wong, T., Leroy, A. K., Walter, F., Bigiel, F., Rosolowsky, E., Fisher, D. B., Vogel, S. N., Blitz, L., West, A. A., & Ott, J. 2012, *ApJ*, 745, 183
- Saintonge, A., Kauffmann, G., Kramer, C., Tacconi, L. J., Buchbender, C., Catinella, B., Fabello, S., Graciá-Carpio, J., Wang, J., Cortese, L., Fu, J., Genzel, R., Giovanelli, R., Guo, Q., Haynes, M. P., Heckman, T. M., Krumholz, M. R., Lomonias, J., Li, C., Moran, S., Rodríguez-Fernandez, N., Schiminovich, D., Schuster, K., & Sievers, A. 2011a, *MNRAS*, 415, 32
- Saintonge, A., Kauffmann, G., Wang, J., Kramer, C., Tacconi, L. J., Buchbender, C., Catinella, B., Graciá-Carpio, J., Cortese, L., Fabello, S., Fu, J., Genzel, R., Giovanelli, R., Guo, Q., Haynes, M. P., Heckman, T. M., Krumholz, M. R., Lomonias, J., Li, C., Moran, S., Rodríguez-Fernandez, N., Schiminovich, D., Schuster, K., & Sievers, A. 2011b, *MNRAS*, 415, 61
- Swinbank, A. M., Smail, I., Sobral, D., Theuns, T., Best, P. N., & Geach, J. E. 2012, *ApJ*, 760, 130
- Swinbank, A. M., Webb, T. M., Richard, J., Bower, R. G., Ellis, R. S., Illingworth, G., Jones, T., Kriek, M., Smail, I., Stark, D. P., & van Dokkum, P. 2009, *MNRAS*, 400, 1121

- Tacconi, L. J., Genzel, R., Neri, R., Cox, P., Cooper, M. C., Shapiro, K., Bolatto, A., Bouché, N., Bournaud, F., Burkert, A., Combes, F., Comerford, J., Davis, M., Schreiber, N. M. F., Garcia-Burillo, S., Gracia-Carpio, J., Lutz, D., Naab, T., Omont, A., Shapley, A., Sternberg, A., & Weiner, B. 2010, *Nature*, 463, 781
- Tacconi, L. J., Neri, R., Genzel, R., Combes, F., Bolatto, A., Cooper, M. C., Wuyts, S., Bournaud, F., Burkert, A., Comerford, J., Cox, P., Davis, M., Förster Schreiber, N. M., García-Burillo, S., Gracia-Carpio, J., Lutz, D., Naab, T., Newman, S., Omont, A., Saintonge, A., Shapiro Griffin, K., Shapley, A., Sternberg, A., & Weiner, B. 2013, *ApJ*, 768, 74
- Toomre, A. 1964, *ApJ*, 139, 1217
- van der Kruit, P. C., & Freeman, K. C. 2011, *ARA&A*, 49, 301
- Wisnioski, E., Glazebrook, K., Blake, C., Poole, G. B., Green, A. W., Wyder, T., & Martin, C. 2012, *MNRAS*, 422, 3339
- Wisnioski, E., Glazebrook, K., Blake, C., Wyder, T., Martin, C., Poole, G. B., Sharp, R., Couch, W., Kacprzak, G. G., Brough, S., Colless, M., Contreras, C., Croom, S., Croton, D., Davis, T., Drinkwater, M. J., Forster, K., Gilbank, D. G., Gladders, M., Jelliffe, B., Jurek, R. J., Li, I.-H., Madore, B., Pimblet, K., Pracy, M., Woods, D., & Yee, H. K. C. 2011, *MNRAS*, 417, 2601
- York, D. G., & SDSS Collaboration. 2000, *AJ*, 120, 1579
- Young, J. S., & Scoville, N. Z. 1991, *ARA&A*, 29, 581